International Union of Crystallography

Commission on Charge, Spin and Momentum Densities.

Comparison of Experimental Methods for Measuring Electron Momentum Distributions

By W. A. Reed, *Bell Laboratories, Murray Hill, New Jersey* 07974, *U.S.A.*

A comparison and evaluation is presented of four experimental methods for measuring electron momentum distributions. The methods considered are photon Compton scattering, electron Compton scattering, $(e, 2e)$ and positron annihilation. This report was prepared at the request of the IUCr Commission on Charge, Spin and Momentum Densities.

I. Introduction

In 1973 the Special Commission on Charge, Spin and Momentum Densities requested a comparison and evaluation of the various techniques used experimentally to measure electron momentum distributions. This report is an attempt to fill that request. The emphasis is on evaluation and comparison of the various methods and not on detailed descriptions of either the theoretical foundations or the experimental techniques since such descriptions exist in the literature.

There are many experimental techniques which provide either direct or indirect information about the momentum distributions of electrons in gases, liquids and solids. However, in this report the discussion is confined to those experimental techniques which measure the momentum density

$$n(\mathbf{p}) = |\chi(\mathbf{p})|^2 , \qquad (1)$$

where $\chi(\mathbf{p})$ is the electronic wave function in momentum space. $\chi(\mathbf{p})$ can be related, through the Fourier transform, to the real-space wave function $\psi(\mathbf{r})$, which is the function usually calculated,

$$\chi(\mathbf{p}) = \int \Psi(\mathbf{r}) \exp (i\mathbf{p} \cdot \mathbf{r}) d^3 r . \qquad (2)$$

Because this group of experimental techniques provides a direct a test of the electron wave function in not only metals, but also in other solids, in atoms and in molecules, it is currently of great interest.

The number of experimental techniques discussed in this report is thus limited to four [photon Compton scattering, positron annihilation, electron Compton scattering and $(e, 2e)$ electron scattering] since they are considered to be the major methods of measuring electron momentum distributions. Other techniques are not discussed since they have made limited contributions to our knowledge of momentum distributions. In addition, the discussion of the experimental apparatus is limited to its application in determining momentum densities, even though the apparatus may be useful for a variety of other measurements.

II. Photon Compton scattering

II A. Introduction and theory

By the end of the 1930's it was recognized that photon Compton scattering could provide information about electron momentum distributions. Unfortunately, the field

lay dormant until the 1960's when interest was revived by improvements in both the theory and experimental methods.

The use of Compton scattering to measure momentum distributions in real materials depends basically on the validity of the impulse approximation. If it were necessary to know both the initial and final states of the scattered electron it would be essentially impossible to interpret experimental data. However the impulse approximation assumes that the electron–photon interaction time is short and the electron is given sufficient energy to excite it into the continuum so that the final state of the electron can be taken to be a plane wave. Platzman & Tzoar (1965) demonstrated the validity of this approximation for free electrons and then Eisenberger & Platzman (1971) showed that the impules approximation is also valid for bound electrons, as long as the electron's recoil energy is much larger than its binding energy.

The calculation of the scattering cross section can be made either in the non-relativistic limit (Platzman & Tzoar, 1965) or in some form of relativistic approximation (Eisenberger & Reed, 1974; Ribberfors, 1975). A comparison of the cross sections shows that the magnitudes are significantly different but the *energy dependence* of the cross section is essentially the same in the energy range of practical interest. Thus both approximations make about the same correction to the experimental data.

The relativistic form of the differential cross section is given by (Eisenberger & Reed, 1974)

$$\frac{d\sigma}{d\omega d\Omega} = \frac{r_0^2 mc\omega_2 \bar{X}}{2\omega_1 \left[(\omega_1^2 + \omega_2^2 - 2\omega_1\omega_2 \cos \theta^{1/2} + \dfrac{q}{mc} (\omega_1 - \omega_2) \right]} J(q) , \qquad (3)$$

where

$$\bar{X} = \frac{\omega_1(1 + q/mc)}{\omega_2(1 - q/mc)} + \frac{\omega_2(1 - q/mc)}{\omega_1(1 + q/mc)} , \qquad (4)$$

$$J(q) = \int_{-\infty}^{\infty} \int_{-\infty}^{\infty} n(\mathbf{p}) dp_x dp_y ,$$

$$q = \frac{(\mathbf{k}_1 - \mathbf{k}_2) \cdot \mathbf{p}_0}{|\mathbf{k}_1 - \mathbf{k}_2|} = 137 \frac{\omega_1 - \omega_2 - \omega_1\omega_2(1 - \cos \theta)/mc^2}{(\omega_1^2 + \omega_2^2 - 2\omega_1\omega_2 \cos \theta)^{1/2}} , \qquad (5)$$

and q is taken parallel to p_z. The energies and momenta of the incident and scattered photons are denoted by $\omega_1, \mathbf{k}_1$ and $\omega_2, \mathbf{k}_2$ respectively and $\hbar = 1$.

To test experimentally the validity of the approximations, Eisenberger (1970, 1972) has measured simple systems for which good electron wave functions are available. The agreement in all cases is less than the experimental error with the possible exception of H_2. It is therefore concluded that as long as the experimental measurements meet the condition of the approximations, Compton scattering data can be interpreted in terms of electron momentum distributions. However, it is possible that for low-energy incident photons and/or samples of high atomic number impulse corrections may be required for the core electrons.

II B. Experimental descriptions

1. *X-ray methods.* Essentially all photon Compton scattering experiments before 1970 were performed using X-rays. A typical experimental arrangement is shown in Fig. 1. The scattered radiation is collimated by slit 1, energy analyzed by the LiF crystal and collimated again by slit 2 before being counted by a scintillation detector. After collecting the desired number of counts at a given energy, the analyzer crystal is rotated to a new angle and data are collected at a new energy. Thus as the energy is stepped, data are collected across the profile. Since counting rates are generally low, especially for samples with large atomic numbers the equipment is usually automated so that many passes through the energy region of interest can be performed and the desired statistical accuracy achieved.

The resolution of the spectrometer is controlled by the size of the slits 1 and 2. Although a resolution of 1 eV or better can be obtained, practical limitations due to the low counting rates require that a resolution of about 50 eV be used. This corresponds to a resolution of about $q = 0.3$ a.u. FWHM for a profile centered at 15 keV using Mo radiation (17 keV). Detailed descriptions of this method can be found in Eisenberger (1970, 1972), Phillips & Weiss (1968) and Cooper (1971).

To analyze the data one must correct for (a) energy dependence of the cross section, (b) sample absorption, (c) spectrometer resolution, (d) multi-energy input radiation and (e) background, and (f) convert from an energy to a momentum scale. Corrections (a), (b) and (f) are straightforward and (c) presents no major problem although care must be taken in measuring the resolution function and
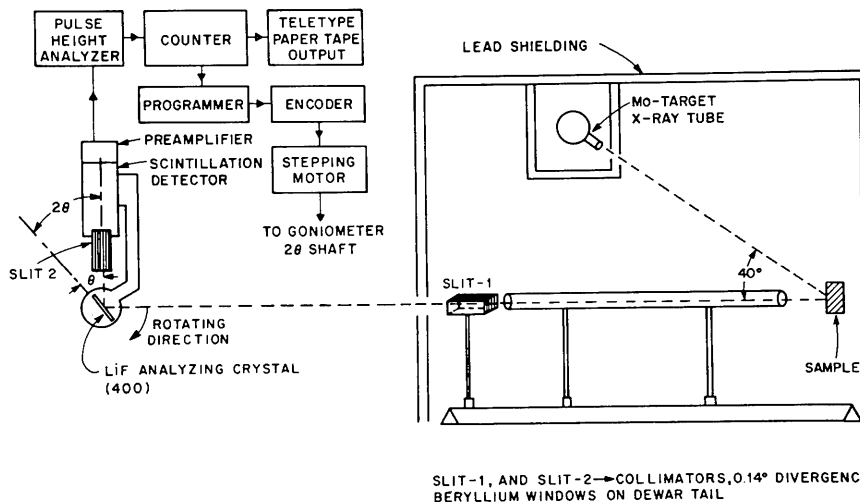

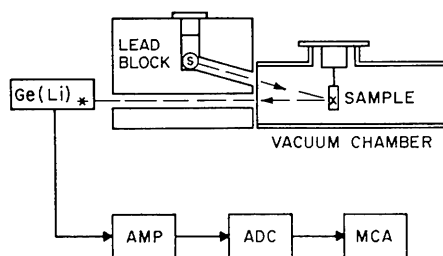Fig. 2. Schematic diagram of a typical Compton scattering spectrometer using a γ-ray source.

performing the deconvolution. The deconvolution problem will be dealt with in more detail later in this report. The data is then normalized such that

$$\int_{-\infty}^{\infty} J(q)dq = \frac{1}{T} \int_{-\infty}^{\infty} C(q)dq = N,$$

where J is the Compton profile, C is the corrected data in counts, T is the normalization constant and N is the number of electrons per unit cell of the sample.

Correction (d) is required because the X-ray source emits a bremsstrahlung background and a $K\alpha_1, K\alpha_2$ doublet. The problem of the $K\alpha$ doublet is treated by the Rachinger (1968) method which is used to remove the $K\alpha_2$ component. The effect of the bremsstrahlung radiation and random background is usually removed by assuming that at some value of $q \geq q_c$ the profile is only due to core electrons. A constant background is then subtracted from the data until for $q > q_c$ the measured profile agrees with a core profile calculated from atomic wave functions (Weiss, Harrey & Phillips, 1968).

2. *γ-ray methods.* In the late 1960's improvements in solid-state detectors led to their use, in conjunction with γ-ray emitting radioactive sources, in measuring Compton profiles. Germanium detectors are generally used, either 'intrinsic' or 'lithium drifted' [Ge(Li)], rather than silicon due to their higher efficiencies at energies greater than 50 keV. Currently typical resolution specifications for both types of Ge detectors are less than 200 eV for 5.9 keV photons (^{55}Fe) and less than 500 eV for 122 keV photons

SLIT-1, AND SLIT-2→COLLIMATORS,0.14° DIVERGENCE
BERYLLIUM WINDOWS ON DEWAR TAIL

Fig. 1. Schematic diagram of a typical Compton scattering spectrometer using an X-ray source.

(^{57}Co) Fig. 2 shows schematically a typical γ-ray experiment. The source is placed in a lead block or some other shield, and the radiation collimated to shine on the sample. The photons Compton scatter at a predetermined angle (e.g. 150 to 175°), pass through a second collimator and are counted by the detector. The counts are amplified, converted to a digital format (ADC), and recorded as a function of energy in a multichannel analyzer (MCA).

The raw data, $M(E)$, are then corrected such that

$$C(E) = G(E)X(E)A(E)\,[M(E) - B(E)]\,,$$

where: $B(E)$ is the background, $A(E)$ is sample absorption, $X(E)$ is the Compton cross section and $G(E)$ is the efficiency of the detector. As indicated, each is a function of energy. The corrected data is deconvoluted with the resolution function, $R(E)$ and then normalized such that the area under the Compton profile equals the number of electrons per unit cell of the sample. Before the normalization step the energy scale must be converted to a momentum scale. We therefore have

$$\int_{-\infty}^{\infty} J(q)\mathrm{d}q = \frac{1}{T} \int_{-\infty}^{\infty} [C(E) \otimes R(E)]\mathrm{d}E\,\frac{\mathrm{d}q}{\mathrm{d}E} = N \text{ electrons}\,,$$

$$(6)$$

where T is the normalization constant. The background function is measured independently and scaled for each measurement since the functional form remains constant. The Compton cross section has been calculated in both the non-relativistic (Platzman & Tzoar, 1965) and relativistic (Eisenberger & Reed, 1974; Ribberfors, 1975; Manninen, Paakkari & Kajantie, 1974) limits but as noted by Williams (1976) the effective difference is small since the q dependence is similar. As a result of the normalization condition only the energy dependence of the factors G, X and A needs to be known and not their absolute magnitudes. Detailed descriptions of the data handling methods are contained in Paatero, Manninen & Paakkari (1974) and Eisenberger & Reed (1972).

The γ-ray sources currently in use are ^{241}Am which emits a 59·57 keV γ-ray and ^{123m}Te which emits a 159·0 keV γ-ray. Each source has certain advantages and disadvantages.The advantages of the Am are a long half-life (458 a) so that source strength remains essentially constant and frequent replacement is not necessary, and the Ge detector efficiencies are essentially 100% in the energy range over which the Compton measurements are made (roughly between 45 and 60 keV). One disadvantage is that only ~30% of the radiation is emitted as the 59 keV γ-ray and self absorption is high so that point radiation sources of high intensity are effectively impossible. For example a cylindrical source ~6 mm in diameter and 1·12 cm deep has a total strength of ~1·3 Ci but only ~0·3 Ci is emitted at 59 keV along the cylinder axis. A second disadvantage is that for 59 keV photons the ratio of photoelectric-to-Compton cross sections (Eisenberger & Reed, 1972) becomes greater than one for atomic numbers greater than ~15. Thus measurement times are significantly longer for Am sources compared to the Te sources. The advantages of the Te sources are a greater penetration of the sample by the higher-energy photons and a more favorable photoelectric-to-Compton cross-section ratio, the impulse approximation is valid for more elements since the electrons have a higher recoil energy, (Eisenberger & Reed, 1972, 1974) and the width of the Compton profile (centered at ~98 keV) relative to the detector resolution is greater than for the Am sources. The

disadvantages are the initial cost of the source is high (~$6000/Ci, in 1974) and available from only a few suppliers (such as the Oak Ridge Laboratory in Tennessee, U.S.A.), the half-life of this source is 120 d so that it must be reactivated every 6 months to a year, and because the profile occurs above ~60 keV, the energy dependence of the detector efficiency factor $G(E)$ is large. This last point is important since a small systematic error in G can have a large effect on $J(q)$ due to the way $J(q)$ is normalized [equation (6)].

With the possibility that synchroton radiation sources will be available in the near future with energies of the order of 10^2 keV, one will not be restricted to a few selected energies. The optimum conditions for such experiments using solid-state detectors has been discussed by Fukamachi & Hosoya (1973).

Two interesting variations of Compton scattering have been published.

The first is the separation of profiles of each atomic level by coincidence detection of the Compton photon and the emitted fluorescent photon characteristic of the level under study. Fukamachi & Hosoya (1972) have published results on the 1s electrons in Fe, Cu, and Ni. In principle this is a great idea but in practice this technique has certain problems which have not been solved. To illustrate the problem consider the measurement of a 1s electron. The incident photon Compton scatters from a 1s electron, an electron drops to fill the 1s hole and emits, for instance, a $K\alpha_1$ photon. Since the coincidence conditions are satisfied a count will be recorded. However a fraction of the scattered electrons will have sufficient energy to eject a second 1s electron with the subsequent $K\alpha_1$ photon emitted. There is a good probability that some photon will enter the Compton detector in coincidence with the spurious $K\alpha_1$ photon and be recorded as a valid count. In fact the ejected electron which causes a $K\alpha_1$ photon can be the result of photons scattering from any of the electrons. Thus there is a mechanism for collecting counts from photons scattered from electrons other than the 1s level. Even though the extra counts may be only 5–10% of the total, this is enough to make the final results of minimal interest. If these problems can be solved however, this method could prove to be extremely useful, especially in the study of molecular systems.

The second variation is the attempt by Hosoya (1974) and co-workers to test a theory of Platzman & Tzoar (1970) which showed that the Compton scattering cross section for circularly polarized photons from a magnetic material was different depending upon the direction of magnetization. In his review talk Hosoya (1974) reported some preliminary results which indicate that the effect is measurable. However more measurements are needed before any firm conclusion can be reached about the usefulness of the variation.

II C. General comments and evaluation

It is generally considered by most workers in the field that except for special situations, the γ-ray method is a faster and more accurate way of measuring Compton profiles. The lower input energy of the photons, the uncertainties in removing the background, the limitation of having to measure the profile one point at a time puts the X-ray method at a distinct disadvantage. Only for special cases where scattering intensity is no problem and ultra-high resolution is desired would X-rays be considered. The possible exception to this statement might be where a

synchrotron is used as a source. However the use of synchrotron radiation in Compton scattering experiments has only just started.

The choice between using an Am or Te source is more difficult. For most studies Am is more than adequate and the cost and availability of this source are distinctly in its favor. However, to measure some of the more interesting materials made up of transition elements, the higher-energy photons of the Te source are an advantage.

The most serious problem plaguing Compton experiments is multiple scattering. Although the majority of the photons detected have only scattered once, a significant number of photons detected have scattered from two or even three electrons. In some circumstances 25% of the recorded photons have been multiply scattered. The effect of multiple scattering is to broaden the profile and decrease the value of $J(0)$. Experimentally there is no way to eliminate completely multiple scattering in a single measurement, but some attempts have been made to measure the profile as a function of thickness and then extrapolate the data to zero thickness. If two samples are both reasonably thin (compared to the penetration depth) then a linear extrapolation is reasonably good. Recently, considerable progress has been made in developing theoretical methods for removing multiple scattering effects from the data. (Felsteiner, Pattison & Cooper, 1974; Pattison, Manninen, Felsteiner & Cooper, 1974; Felsteiner & Pattison, 1975; Williams & Halonen, 1975). Monte Carlo programs have been written which seem to do remarkably well. With the perfection of this type of correction, multiple scattering should cease to be a significant problem.

Basically the types of information gained from Compton measurements are the averaged profile $J(q)$ for a polycrystalline, powdered, liquid or gaseous sample; the $J(q)$ for a specific crystallographic direction on a single crystal, and the variation of $J(q)$ with crystallographic direction. The best measurements published to date have an accuracy of about 1–2% for the total profiles and about 0·5% for anisotropy measurements. In addition to counting statistics, there are additional errors associated with the various corrections made to the data. These errors are discussed in detail by Williams (1976).

II D. Summary

γ-ray Compton scattering is probably the easiest of the various methods used to measure electron momentum distributions. It can produce accurate data, on all types of samples, which provide sensitive tests of theoretical wave functions. Its biggest problem compared to the other techniques is the relative lack of resolution.

III. High-energy electron Compton scattering

III A. Introduction and theory

As in the case of Compton scattering, inelastic electron scattering was studied in the 1930's by Hughes & Mann (1938) and then essentially neglected until the late 1960's when a combination of experimental and theoretical advances revived the field.

Detail discussions of the theory of inelastic electron scattering are given by Bonham & Tavard (1973), Lassettre & Skerbela (1974), Bonham & Fink (1974), Ionkuti (1971), Tavard & Bonham (1969), Bonham (1969), Bonham & Wellenstein (1973a), with Bonham & Fink (1974) giving the most recent and detailed treatment. These papers show

that there are basically two theoretical assumptions and two corrections which affect the scattering cross section.

The first Born approximation is the basic assumption in the calculation of the cross section. This approximation assumes that the electron is scattered by only one point in the potential field and thus the differential cross section can be written as a product of the Rutherford cross section times the energy derivative of the generalized oscillator strength (Ionkuti, 1971). This approximation (Bonham & Fink, 1974) is best for small atoms and molecules; however, calculations show that for 40 keV electrons elastically scattered from Ar the approximation is valid to better than 5% when compared to rigorous estimates. It is expected that the Born approximation is at least as good for inelastic scattering.

After the Born approximation, the second assumption in the calculation of the differential cross section is the binary encounter approximation. This is analogous to the impulse approximation for photon–electron scattering and essentially assumes that the interaction is between only two electrons, the momentum transferred to the target electron is large (compared to the binding energy), and the time of electron–electron interaction is short enough that the potential can be considered a constant. This allows the final state of the electron to be taken as a plane wave which in turn allows the differential scattering cross section to depend only on the ground state of the system. Experimentally, if the binary encounter approximation is found to be valid, this implies the validity of the Born approximation.

There are two corrections which are made to the cross section calculated using the above assumptions. The first is for relativistic effects. There appears to be no special problem with this correction which amounts to $< 1\%$ for 25 keV electrons and $< 2\%$ for 50 keV electrons at scattering angles of about 10°. The second correction is for exchange and interference of the incident and scattered electrons. These corrections can be quite large ($\sim 25\%$) but by properly selecting the scattering angle they can be minimized. At high incident electron energies this correction depends only on the scattering angle and is less than 2% for angles smaller than 10°.

The net result of these calculations leads to a differential cross section given by (Wellenstein & Bonham, 1973; Wellenstein, Bonham & Ulsh, 1973).

$$\frac{d^2\sigma}{d\Omega dE} = \frac{2k_s[1 - E(1-\beta^2)^{1/2}/2c^2]}{k_i(1-\beta^2)[K^2 - E^2/4c^2]^2} F_{ex}J(q),\quad (7)$$

where $\mathbf{k}_i$ and $\mathbf{k}_s$ are the wave vectors of the incident and scattered electrons, $\mathbf{K}$ is the momentum transfer $(\mathbf{k}_i - \mathbf{k}_s)$, $q = [E(1 - E/4c) - K^2]$ and E is the energy loss on scattering. The exchange and interference corrections are approximated by

$$F_{ex} \simeq 1 - \frac{K^2}{k_s^2} + \frac{K^4}{k_s^4} + \frac{2K^4q^2}{k_s^6},\quad (8)$$

and the $J(q)$ term is the Compton profile and given by

$$J(q) = 2\pi \int_q^\infty n(p)p\,dp$$

(isotropic momentum distribution).

Although there are three possible ways to convert the experimental measurements to an absolute scale (Bonham & Tavard, 1973), only two of these are normally used. The first method involves a sum rule by Bethe which states that all the generalized oscillator strengths should sum to N, the

number of electrons in the system. The second method is simply the requirement that the integral of $J(q)$ over all q must equal N. These two methods are equivalent if the binary encounter approximation is valid but the second method will fail as the binary encounter approximation fails. Thus the validity of this approximation may be tested under the actual experimental conditions. The third method, which uses the ratio of the elastic to the inelastic differential cross section, is seldom used in practice.

III B. Experimental description

Although there are several groups investigating the physics of high-energy electron scattering, the groups under the direction of R. A. Bonham at Indiana University and H. F. Wellenstein at Brandeis University are most actively pursuing the use of this technique to study electron momentum distributions. Therefore the description of apparatus and experimental results will be based largely on their work. (Wellenstein & Bonham, 1973; Bonham & Wellenstein, 1975b).

The apparatus used to measure gaseous samples is shown in Fig. 3 and described by Wellenstein, Schmoranzer, Bonham, Tuck & Lee (1975). The large chamber is evacuated with a 20 kl/s pump to a pressure of $\sim 10^{-7}$ torr with no sample present and $\sim 10^{-5}$ torr with a sample. It is made of nonmagnetic material and shielded from magnetic fields. The sample is injected as a gas through a hypodermic needle ~ 0.12 mm i.d. and 5 mm long at a flow rate of 10^{18} to 10^{20} atoms or molecules/s. A collimated beam of electrons (Schmoranzer, Wellenstein & Bonham, 1975), whose energy can be varied from 18 to 50 keV, strikes the sample where the jet is approximately 0.5 mm wide (Bonham & Wellenstein, 1973b). The beam is ~ 200 μm FWHM for currents between 0.1–500 μA. The scattered electrons are energy-analyzed by a Möllenstedt velocity analyzer and counted by a Si solid-state detector (Wellenstein, 1973). Data are collected by signal averaging, typically sweeping over 1 keV in a time of 60 s. Sweeps up to 2.4 keV at a rate of 8 min/sweep are now routine. The distance between the scattering volume and the analyzer is ~ 60 cm and a double slit system is used essentially to eliminate background scattering. The energy resolution of the analyzer can be varied between 0.20–20 eV in this range of incident electron energy but due to the energy spread in the incident beam, the optimum resolution is found to be ~ 0.6 eV FWHM. For the measurement of electron momentum distributions, a resolution of 2–5 eV is typically used (~ 0.01–0.03 a.u.). The scattering angle is varied from 0–140° by rotating the electron gun. The relatively large electron–electron scattering cross section and high beam currents make the time for collecting data quite short. Typically for He or H_2 a Compton profile with 10^4 counts in the peak can be collected in less than five minutes. For heavier elements the time required to collect the same number of counts at the same scattering angle is reduced by the ratio of the atomic numbers. However, to satisfy binary encounter conditions, a larger angle is required which severely reduces the count rate.

There are a number of corrections which must be made to the data to convert it into a Compton profile. These corrections with their approximate size are (a) dead-time corrections to the intensity (1–10%), (b) the subtraction of a constant background (less than 0.4% of peak), and (c) a Kollath correction (Kollath, 1936; Wellenstein, 1973) for scanning the spectrum over the entrance slit of the detector

(1%). The theoretical corrections, previously mentioned, are: (d) exchange scattering (1–5% as the scattering angle varies from 0–15°), and (e) relativistic effects (less than 2% for energies < 50 keV and 5° < θ < 15°). In addition there is the conversion of the second-order cross sections to generalized oscillator strength and the normalization of the raw data to an absolute scale by use of the Bethe sum rule.

Due to the high counting rates statistical accuracy of between 0.1 and 1% is easily obtained. A final accuracy of about 1–2% seems obtainable after all corrections are made.

III C. General comments and evaluation

Both the dead-time and background corrections can be accurately measured. The dead time is measuring by comparing count rates in channels near the elastic and inelastic peaks as a function of beam current and the ratio of the two channels determines the dead time (to within 5%). The background is measured by leaking gas into the chamber and measuring the counting rate without the sample. Likewise the Kollath correction is easily made. These corrections, if applied carefully, should not appreciably effect the accuracy of the final result.

Multiple scattering of the incident electrons can be a serious problem if the density of the sample gets too large. However this problem can be eliminated by measuring low-density samples and taking data as a function of density.

The theoretical corrections are more difficult to evaluate. As the atomic number of the sample increases, larger scattering angles are required to prevent failure of the binary encounter theory. However as the scattering angle increases the exchange corrections increase (Bonham & Tavard, 1973) so that corrections of $\sim 25\%$ are possible at angles of $\sim 35°$. For Ar corrections of $\sim 10\%$ are required at angles of 25° using 40 keV electrons. Thus any errors in calculating the energy and momentum dependence of this correction are potentially significant. Relativistic corrections are small ($< 2\%$ for energies < 50 keV) so that any errors due to the approximations made in the relativistic calculation should have a negligible effect on the final profile.

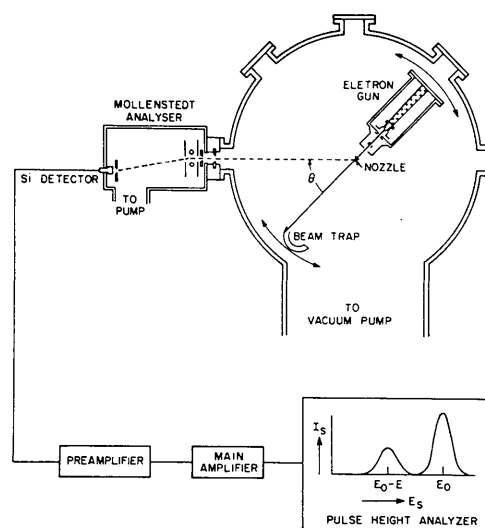As mentioned earlier one of the basic assumptions made

Fig. 3. Schematic diagram of a spectrometer used in high-energy electron Compton scattering.

in calculating the inelastic scattering cross section is the first Born approximation. This approximation is expected to be valid for electron energies above ~ 20 keV and should improve as the energy is increased. Experiments on H_2, N_2 and He show that the data are dependent only on the momentum transfer K for $25 < E < 45$ keV and $1° < \theta < 10°$. This sole dependence on K is regarded as a necessary but not sufficient condition for the Born approximation. Thus the experimental evidence is that the Born approximation is valid to at least 0.5% for light elements in this range of incident electron energies (Bonham & Wellenstein, 1975a).

The binary encounter theory must also be tested to ensure its validity under the experimental conditions. It is possible to test the theory in two ways. The first is to repeat the measurements at a larger scattering angle. If the two profiles agree then the binary encounter theory is valid (assuming the angular dependence of the exchange correction is accurately known). The second method is to integrate the Compton profile.

$$\int_{-\infty}^{\infty} J(q)\mathrm{d}q = N' \ .$$

A value of N' less than N, the number of electrons in the sample, indicates a failure of the binary encounter approximation. Bonham & Wellenstein (1975a) have shown that for electron energies in the range 25–50 keV H_2, D_2, He and N_2 can be measured at $\theta = 12°$ but not for systems containing elements heavier than Ne. These tests also show that the binary encounter limit for the *valence* electrons of N_2 is reached at $\theta \sim 3$–$4°$ with an accuracy level of 4–5%. Langhoff & Seidman (1974) have shown how to make the binary encounter corrections for He-like cores so that it may be possible to measure the total Compton profiles for the first row elements by applying corrections to data taken at angles of 10–12°.

Two additional experimental problems which need to be considered are the calculation of the energy loss scale and the measurement of the scattering angle. The energy scale is calibrated by biasing the accelerating potential by a known voltage and measuring the elastic line. Recording data every 50 eV and curve fitting the results, the channel number-to-energy relationship can be measured to better than 0.5 eV. The scattering angle is measured with a potentiometer coupled to the electron gun. The zero angle is found by scanning the beam across the Faraday trap with a 20 μm entrance hole. The present angular accuracy is $\pm 0.02°$ but could be improved by an order of magnitude (Bonham & Wellenstein, 1975a).

III D. Summary

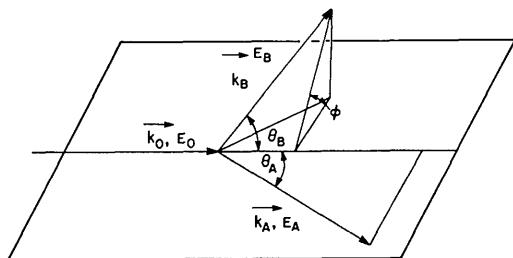At present the use of high-energy electrons to measure electron momentum distributions is limited to gaseous samples of first-row elements. Within this restricted range of samples the method appears to be superior to other methods in terms of attainable statistical accuracy, energy resolution and the elapsed time needed to carry out the experiment. It is possible that this method can be extended to elements beyond the first row of the periodic table. In addition it may also be possible to derive Compton scattering information from electron scattering through thin films or from small crystals by use of selected area diffraction with an electron microscope. These possibilities are as yet largely unexplored and further work is needed to prove their viability.

IV. (e,2e) Method

IV A. Introduction and theory

To measure the Compton profile using photons or electrons only the scattered photon or electron is detected and energy analyzed. The information carried by the recoil electron is lost. However in the experimental method which has become known as '$(e,2e)$', an electron is scattered from the sample and both the scattered and recoil electrons are detected in coincidence. Some initial measurements have been reported by Ehrhardt, Schulz, Takoat & Willman (1969), Ehrhardt, Hesselbacher, Jung & Willman (1972), Camilloni, Giardini-Guidoni & Tiribelli (1972), and Wiel & Brion (1972) but the bulk of the published work to date is by E. Weigold and I. E. McCarthy and their co-workers at Flinders University who have developed the experimental and theoretical techniques necessary to demonstrate the validity of the $(e,2e)$ method for measuring electron momentum distributions.

The basic geometry of the $(e,2e)$ method is shown in Fig. 4. An incoming electron with momentum k_0 and energy E_0 knocks out an electron and the two electrons with momenta k_A, k_B and energies E_A, E_B are detected in coincidence. Thus one can measure the coincidence counting rate as a function of the parameters E_0, E_A, E_B, θ and φ. The usual geometries are (a) to fix $\theta_A = \theta_B$, $E_A = E_B$ and vary φ (non-coplanar symmetric geometry) and (b) to set $\varphi = 0$, $E_A = E_B$ and vary $\theta = \theta_A = \theta_B$ (symmetric coplanar geometry). A third mode of operation is to fix the angles and energies E_A and E_B ($E_A = E_B$) and vary E_0. This mode permits the identification of the various electron orbitals so that the momentum density of each orbital can be measured. This mode is the electron impact equivalent of ESCA or photo-electron spectroscopy.

The approximation developed for the interpretation of the experimental results is called the 'distorted wave off shell impulse approximation' (Hood, McCarthy, Teubner & Weigold, 1973; Furness & McCarthy, 1973, 1974; McCarthy, 1973). It assumes that the incoming electron and the two ejected electrons can be approximated by slightly distorted plane waves and the distortion can be calculated in the eikonal approximation. The differential cross section is then calculated to be

$$\frac{\mathrm{d}\sigma}{\mathrm{d}\Omega_A\mathrm{d}\Omega_B\mathrm{d}E_A} = Nb_{nl}^2 \left(\frac{2me^2}{\hbar^2}\right) \frac{2\pi\eta}{[\exp(2\pi\eta)-1]}$$

$$\times \left\{ \frac{1}{|k-k'|^4} + \frac{1}{|k+k'|^4} - \frac{1}{|k-k'|^2|k+k'|^2} \right.$$

$$\left. \times \cos\left[\eta \ln\left(\frac{|k+k'|^2}{|k-k'|^2}\right)\right] \right\} |\chi_{nl}(K)|^2 \ , \qquad (9)$$

where b_{nl} is the spectroscopic factor,

Fig. 4. Experimental arrangement for $(e,2e)$ measurements.

$$N = \exp\left[-(k_0\gamma_0 + k_A\gamma_A + k_B\gamma_B)R_N\right],$$
$$\eta = me^2/\hbar^2 k',$$
$$\mathbf{k} = (\mathbf{K}_0 - \mathbf{K}), \quad \mathbf{k}' = (\mathbf{K}_A - \mathbf{K}_B),$$
$$\mathbf{K} = \mathbf{K}_0 - \mathbf{K}_A - \mathbf{K}_B,$$
$$\mathbf{K}_i = (1 + \beta + i\gamma)\mathbf{k}_i, \quad i = 0, A, B,$$

and the subscripts $0, A, B$ denote the incoming and the two outgoing electrons. The wave function $\chi(\mathbf{K})$ is the Fourier transform of the ejected electron. More generally, when the effects of electron correlation and the non-orthogonality of the atom and ion wave function are taken into account the single-particle wave function must be replaced by the overlap integral $\langle\psi_{atom}|\psi_{ion}\rangle$, which is a function only of the coordinate of the ejected electron. To calculate the differential cross section it is necessary to evaluate the amplitude of the break-up matrix element. This element contains the distorted waves

$$\Phi_j^{(\pm)}(\mathbf{k},\mathbf{r}) \exp(\pm i\gamma k R_{N_c} i \mathbf{K}_j \mathbf{r}),$$

where R_N is a normalization parameter that ensures $|\Phi_j^{(+)}|$ = 1 just before the electron enters the interaction region.

Thus in this approximation the calculation reduces to determining the three parameters: a wave number modification β, an attenuation constant γ, and a normalization distance R_N. The first two are calculated from (Hood et al., 1973; Furness & McCarthy, 1974; Ugbabe, Weigold & McCarthy, 1975)

$$\beta + i\gamma = \bar{V}/2E,$$

where $\bar{V}$, the complex potential in the interaction region, is determined from experimental electron elastic scattering cross sections. The values of β and γ calculated for loosely bound electrons are found to be small. For example the values for the $3p$ electrons in argon (Hood et al., 1973) are $\beta = \gamma = 0.01$ for $E = 800$ eV and $\beta = \gamma = 0.02$ for $E = 400$ eV. Values of R_N are about 1 Å but its value does not need to be known precisely since it only enters into the magnitude of the cross section. It is apparent that if the binding energy of the electron is small and the incident electron energy is

high enough then

$$\Phi_j^{(\pm)}(\mathbf{k},\mathbf{r}) \cong \exp(i\mathbf{k}.\mathbf{r}),$$

and $|\chi(\mathbf{K})|^2$ is given directly.

An examination of equation (9) shows that the cross section is directly proportional to $|\chi(\mathbf{K})|^2$ which is just the momentum density, $n(\mathbf{p})$. This is a distinct advantage of the $(e, 2e)$ method. The three other experimental methods discussed measure a single or double integral of the momentum density so that some details of the density are 'averaged out' and lost.

IV B. Experimental description

Because the $(e, 2e)$ method is the newest and probably least familiar of the four methods to the reader, a more detailed explanation of the apparatus is given. I am indebted to E. Weigold and I. E. McCarthy for the description.

The two experimental arrangements employed (Ugbabe et al., 1975; Weigold, Hood & McCarthy, 1975) are the symmetric non-coplanar geometry, in which $\theta_A = \theta_B =$ constant and the azimuth φ is varied (Fig. 4), and the symmetric coplanar geometry where $\varphi = 0$ and $\theta_A = \theta_B = \theta$ is varied.

The experimental apparatus is shown schematically in Fig. 5. It is mounted on the bottom plate of a metal bell-jar vacuum chamber, consisting of a type 304 stainless steel cylinder 76·1 cm high and 54·5 cm in diameter, sealed at the top and bottom by aluminum plates by means of O-rings. The chamber is pumped by a high-velocity diffusion pump and associated liquid-nitrogen trap through a port in the bottom plate. It is lined on the inside with mu-metal and surrounded by sets of Helmholtz coils, which reduce stray magnetic fields to less than 5 mG within the regions of interest. Non-magnetic materials are used throughout.

Target gases of at least 99·9% purity are admitted to the interaction region through a length of stainless steel tubing of 0·025 cm i.d. by means of a leak valve. In the coplanar geometry the stainless tubing terminates 0·3 cm below an aperture of 0·075 cm diameter which is placed 0·2 cm
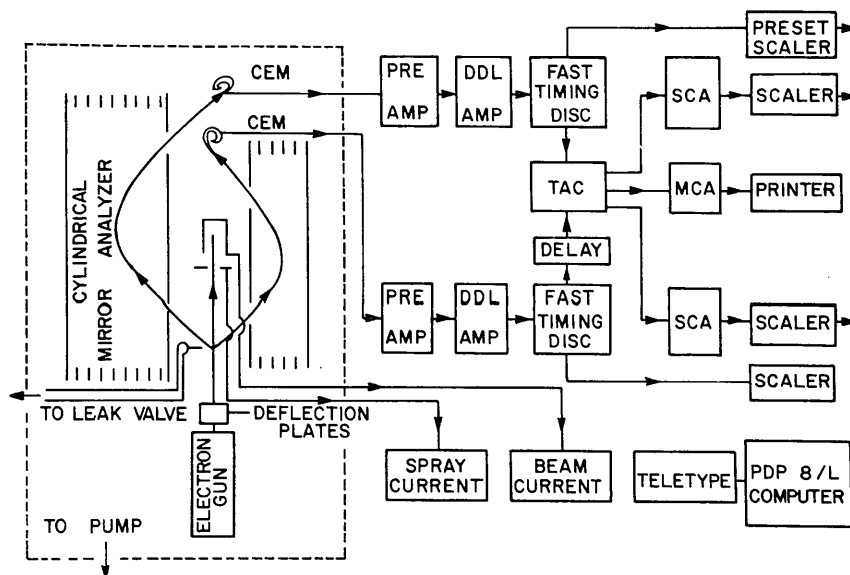

Fig. 5. Schematic diagram of a spectrometer used in $(e, 2e)$ scattering.

below the interaction region. At the leak rates normally employed, this aperture serves to collimate the atomic beam. In the non-coplanar symmetric geometry no aperture is employed. Pressures in the vacuum chamber are $\sim 5 \times 10^{-7}$ torr without a sample and in the range of $\sim 10^{-5}$ torr during the experiments. The pressure on the interaction region is several orders of magnitude higher than the dynamic background pressure which has a long-term stability of a few percent.

The electron beam, provided by a commercial electron gun, is varied in energy between 200 and 1200 eV with currents in the region of 70–200 μA, depending on the energy. During any series of runs the current remains constant to within 1%. A set of deflection plates is used to align the beam with the interaction region. The beam is focused by maximizing the ratio of the current into a Faraday cup of 0·60 cm diameter to the current in a collector surrounding this cup. This same arrangement is used to measure the width of the electron beam.

Two cylindrical mirror electron energy analyzers are mounted on arms pivoting about the axis defined by the atomic beam. In the coplanar symmetric case the two analyzers can be moved independently, but the angles they subtend with respect to the electron beam are usually kept equal. In the non-coplanar symmetric geometry one spectrometer is fixed, and the other is moved about the azimuth. The two analyzers are of identical construction. Fringing fields are minimized by logarithmically spaced cylindrical rings placed at both ends of the analyzers and joined by stainless steel rods. The rings are connected through a resistor chain running between the negative outer cylinder and the grounded inner cylinder. The entrance angle to the analyzer is defined by three apertures. A decelerating lens placed in front of the spectrometers can be used to increase the energy resolution in the experiment. The acceptance angle of the spectrometers is approximately 3°. The exit aperture of the analyzer is placed on the axis of the cylinders and in front of the channel electron multipliers (CEM) used to detect the electrons. The front faces of CEM's are biased negative by a voltage slightly smaller than that corresponding to the energy of the emitted electrons (E_A). In order to obtain unambiguous coincidence counting rates as a function of angle in the coplanar geometry, the region viewed by the spectrometers is made larger than the source region which is defined by the intersection of the atomic and electron beams.

The signal processing electronics is also shown schematically in Fig. 5. Pulses from the CEM's are passed through preamplifiers then amplified by double delay line (DDL) amplifiers. The amplified pulses are passed through fast timing discriminators triggered in the zero crossing mode. The output from one timing discriminator provides the start pulse for a time-to-amplitude converter (TAC), while the delayed pulse from the second discriminator provides the stop pulse. The output of the TAC is fed to a multichannel analyzer (MCA) used to set up and monitor the experiment and to two single-channel analyzers (SCA). One SCA is set with its window covering the coincidence peak, typically 6 ns with FWHM of the peak being 3 ns. The other SCA is used to record accidental coincidences or background, its window being set wider than the coincidence window in order to provide a truer average background count. To minimize the random coincidence the counting rates must be kept low and the detectors must be shielded from high-frequency pickup.

The electron current is monitored throughout each experiment and remains constant to within a few percent. The ambient pressure is measured by an ion gauge whose output is fed into a voltage-to-frequency converter which provides pulses for the preset scaler. The preset scaler controls the gates on all the other scalers. Thus, to a first approximation, changes in atomic beam intensities are compensated for. In any series of measurements, the energies of the outgoing electrons are kept fixed, and therefore the transmission factor of the spectrometers remains constant.

The experiment is carried out in two modes in the first of which the coincidence rate is measured as a function of binding energy at fixed angles, the second mode being the measurement of the angular correlation at fixed energies. A computer (PDP/8L) is used to control the experiment in the binding energy mode. It sets the electron beam energy, records the counts in the coincidence and background scalers after being triggered by the preset scaler, subtracts background counts from the coincidence counts (taking into account the relative channel widths), calculates the statistical error and restarts the scalers after setting the new beam energy. A cumulative result of counts *versus* energy is thus obtained and displayed on an oscilloscope screen. The computer addresses the electron gun power supply *via* a digital-to-analog converter and, similarly, the oscilloscope. The statistical error for each point can be displayed on request.

For the angular correlation measurements, computer control of the angular setting of one spectrometer is available, and therefore in the non-coplanar symmetric geometry the angular correlation is measured under computer control. This facility is not used in the symmetric coplanar geometry since both spectrometers have to be moved. Instead, both spectrometers are at present turned manually and the coincidence counting rate as a function of angle θ recorded.

The energy resolution of this apparatus only needs to be good enough to separate electrons ejected from states with different binding energies. Since binding energies of outer electrons are ~ 10 eV and the states are separated by energies ≥ 10 eV, the current resolution of ~ 1 eV is reasonable. The angular resolution is $\sim 3°$, which corresponds to a momentum resolution of $\sim 0·1$ a.u. in the energy range 200–800 eV.

The only corrections needed to be made on the raw data are for background (from random coincidences) and for detection efficiency as a function of angle and the resolution of the spectrometer which is small.

The accuracy of this method varies between 1–10% depending upon incident energies, cross sections and practical limits on running time. Although the accuracy is poorer than the other methods discussed, it should be remembered that $n(\mathbf{p})$ is measured and not some integral of $n(\mathbf{p})$. If we consider the accuracy that is obtained for $n(\mathbf{p})$ then all the methods are more or less comparable.

IV C. *Evaluation of method*

The $(e, 2e)$ method is a relatively new method of measuring momentum distribution so that much of its potential is still unrealized. Likewise some of its limitations are probably also unknown. However, based on the current state of the art, it is a powerful technique which offers several unique advantages.

The advantages are (*a*) the momentum density is measured directly, and not an integral of $n(\mathbf{p})$. (*b*) the momen-

tum density of separate electron shells in the atom or molecule may be measured by varying the input energy and (c) the data provide a sensitive test of configuration interaction in the single-particle approximation (Ugbabe et al., 1975; Weigold et al., 1975; McCarthy, Teubner & Weigold, Hood, 1974; Dey, McCarthy, Teubner & Weigold, 1975).

The present limitations of the experimental apparatus described are (a) the samples must be gases, or at least volatile enough to be used in a gaseous state so that only the radial momentum distribution is measured and (b) only the outer electrons can be measured due to low counting rates for the core electrons. However, it should be noted that Camilloni et al. (1972) report measurements of the core electrons in carbon using thin film targets and 9·3 keV incident electrons so that these limitations may only apply at lower incident energies. In comparing theoretical wave functions with experiment, problems can arise since (c) the distortions in the distorted-wave model become greater in heavy atoms and these small errors in calculating the distortions are reflected as errors in the wave function being tested and (d) the comparison between theory and experiment is made by matching them at some point so that only the angular dependence and relative magnitudes are checked and not the absolute magnitude. Points (c) and (d) are probably not serious. The distortions in point (c) become smaller as the incident electron energy is increased and are essentially zero when the apparent momentum distribution becomes energy independent. However the extent to which the incident energy can be increased is limited. As E_0 increases the relevant range of angles decreases and at some point the angular resolution is inadequate. It should also be noted that extensive testing of the distorted wave model shows that it yields accurate results. The need to match the theory and experiment at some arbitrary point is also not critical. First, it is the dependence on q which is important and second, there are other checks possible, such as spectroscopic factors (Hood et al., 1974) which can be used as an additional test.

V. Positron annihilation

V A. Introduction and theory

When a high-energy positron is injected into a sample as a metal it quickly thermalizes and annihilates with an electron. The most probable mode of annihilation is by the emission of two photons. If the electron and positron were at rest these photons would be emitted in exactly opposite directions and each would have an energy mc^2. However if the electron is not at rest and the initial momentum of the electron is included, the angle between the two photons deviates from 180° by $\sim p_T/mc$ where p_T is the momentum component transverse to the emission direction of the two photons. The energy of each emitted photon is $mc^2 \pm cp_P/2$ where p_P is the momentum parallel to the emission direction. Thus measurement of either the two-photon angular correlation or the energy shift of one of the photons will provide information about the initial momentum of the electron. Reviews of positron annihilation have been written by Dekhtyar (1974) and West (1973), which treats all aspects of the subject, and by Berko & Mader (1975) which deals more specifically with the application of this method to Fermi surface studies in metals and alloys. The reader is referred to these papers for more detailed discussions and comprehensive biographies of the subject.

In the approximation of the independent particle model

the probability of annihilation with an electron of initial momentum $\mathbf{p}$ is

$$\varrho(\mathbf{p}) = |\int \exp(-i\mathbf{p} \cdot \mathbf{r})\psi_+(\mathbf{r})\psi_m(\mathbf{r})\mathrm{d}^3r|^2, \qquad (10)$$

where $\psi_+(\mathbf{r})$ is the ground state positron wave function, and $\psi_m(\mathbf{r})$ is the ground state electron wave function. This expression is identical to $n(\mathbf{p})$ derived in Compton scattering if $\psi_+(\mathbf{r}) = \mathrm{const}$. Thus, the two experimental techniques are, in principle, nearly identical. However, as will be seen, real differences exist due to experimental considerations.

The basic theoretical problem in the interpretation of the momentum density as measured by positrons is how to treat the positron wave function $\psi_+(\mathbf{r})$. Due to the repulsion of the positron by the ion cores the annihilation is more likely to occur with a valence electron than with a core electron. Thus the measured momentum distribution emphasizes the contributions of the outer electrons. The contribution of the core electrons can only be known by assuming some form for $\psi_+(\mathbf{r})$. Calculations of $\psi_+(\mathbf{r})$ such as those performed by Berko & Plaskett (1958), Stroud & Ehrenreich (1968) and Mijnarends (1973) which include the crystal potential are becoming better; however these calculations still represent a source of uncertainty when comparing experimental and theoretical momentum distributions.

V B. Experimental description

One of the clearest ways to describe the experimental geometry used in positron annihilation is presented by Berko & Mader (1975) (Fig. 6). A positron annihilates with an electron having momentum $\mathbf{p}$ (double arrow) and the angle between the two emitted photons is $\pi \pm \sim 10^{-3}$ rad. The object of the experiment is to measure, in coincidence, the angular distribution of these photon pairs. To accomplish this a detector (C_1) is placed at $X = -L$ on the axis of the spectrometer. A second detector (C_2) is placed on a plane at $X = +L$ with coordinates $y = L\varphi$ and $z = L\theta$. (Since the angular deviations of the two photons are typically a few milliradians and L is ~ 3–5 m, $y = L\varphi$ to better than 1%). If, in addition, the energy dependence of the photons detected by counter C_1 is measured, p_x is determined and the complete $\varrho(\mathbf{p})$ in (10) is known. However, due to low counting rates and poor energy resolution, the energy determination is not made, so that the coincidence rate is proportional to

$$N(p_y, p_z) = \int_{-\infty}^{\infty} \varrho(\mathbf{p})\mathrm{d}p_x. \qquad (11)$$

This is known as either the 'crossed-slit' or 'point-slit' geometry and measures a line through the momentum distribution (Berko & Mader, 1975; Kim & Buyers, 1972; Nanao, Tanigawa, Kuribayashi & Doyama, 1971). This geometry also restricts the counting rate so that the majority of the angular correlation measurements use the 'long-slit' geometry (Berko & Plaskett, 1958; Gustafson, Makintosh & Zaffarano, 1963). In this configuration the counters are made long in the y direction so that the measurements are proportional to

$$N(p_z) = \int_{-\infty}^{\infty} \int \varrho(\mathbf{p})\mathrm{d}p_x\mathrm{d}p_y. \qquad (12)$$

A typical 'long-slit' apparatus is shown in Fig. 7. The positron source (0·01–0·1 Ci) is usually ^{58}Co, ^{22}Na or ^{64}Cu. It is placed above or below the sample and the magnet (~ 20 kG) focuses the positrons onto the sample. The

detectors are NaI(Tl)-scintillators placed at several meters from the sample and are typically 30 to 60 cm long and 5 cm high. Depending on the details of the spectrometer, the detectors subtend angles of 100–250 mrad by 0·1–0·5 mrad. The coincidence rate is then measured as a function of the angle θ (in steps of $\sim 0·2$ mrad to $\theta_{max} \sim 25$ mrad).* The electronic components used to measure the coincidence need a resolution time of < 50 ns, and are commercially available. It is common to have the spectrometer automated so that the angle is changed after a preset time or number of counts.

The 'crossed-slit' geometry spectrometers are basically the same as shown in Fig. 7 except that additional slits are placed in front of the detectors to limit the beam in the 'y' direction (see Fig. 6). The angular resolution is typically 0·5–1·0 mrad in θ and 1–5 mrad in φ. The coincidence rate in this geometry is greatly reduced so that sources of 1 Ci or more are often used. A novel application of the ^{64}Cu source is in the study of copper and copper-based alloys. The samples are irradiated with neutrons to produce an intense ^{64}Cu source internal to the sample (Fujiwara & Sueoka, 1966).

A variation of the crossed-slit geometry is the 'rotating specimen' method (Sueoka, 1967; Williams, Becker, Petijevich & Jones, 1968). The point counters are kept collinear ($\theta = 0$, $\varphi = 0$) and the sample is rotated about the spectrometer axis. In principle this method should measure the diameter of the Fermi surface of a metal but in practice yields data complicated by contributions from high-momentum components, core anisotropy and enhancement. In this context the core anisotropy is due to the $3d$ electrons and the high-momentum components are due to the inner shells. Until it is understood how to correct for these components and for the contribution of the core electrons, this method will not be of much practical value for the measurement of momentum distributions.

---

* Positron annihilation data are usually presented as a function of θ in the units of milliradians. Since 1 atomic unit of momentum equals $mc\theta$, 1 mrad $= 0·137$ a.u. $= 0·259$ Å^{-1}.
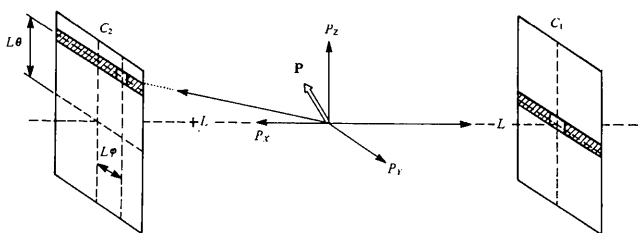

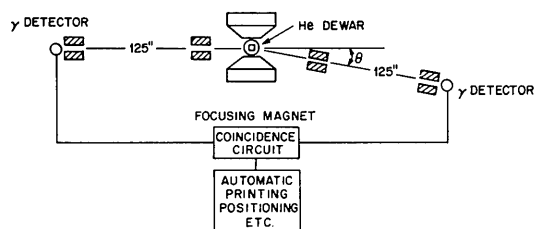Fig. 6. Experimental arrangement for positron annihilation measurements.

Fig. 7. Schematic diagram of a long-slit spectrometer used in positron annihilation measurements.

To regain some of the time lost in the crossed-slit geometry due to decreased counting rates, several schemes have been proposed which increase, or effectively increase, the number of counters. Berko & Mader (1975) have set up an apparatus which uses 11 pairs of counters and Howells & Osmon (1972) have attempted to use a spark chamber to obtain a two-dimensional array of detectors. Berko's method is currently producing data whereas Howells & Osmon's method has not proved practical due to the low efficiency of the spark chamber for γ-rays.

As previously mentioned the x component of momentum (see Fig. 6) can be determined from the energy dependence of the emitted photons. The experimental arrangement is quite simple: (Rama-Reddy & Carrigan, 1970; Hotz, Mathiesen & Hurloy, 1968; Dauwe, Dorikens-Vanpraet & Dorkins, 1972) a positron source is placed next to the sample and the emitted photons analyzed by a Ge(Li) detector. The basic problem with this method is that even the best detectors do not have sufficient resolution ($\sim 1·5$ keV, FWHM) at 510 keV to resolve adequately the details of the momentum distribution (< 3 keV, FWHM). An improvement in resolution of a factor of 5–10 is needed before it could compete with other methods. Also, as pointed out by West (1973), there may be additional advantages and problems which will only appear as this method is investigated in more detail.

V C. Evaluation of method

Only the angular correlation method using either long-slit or crossed-slit geometries has been shown capable of producing precise data on momentum distributions. The coincidence electronics presents no problems and the resolution is excellent. The only corrections one must make to the raw data are (a) the subtraction of random counts which is typically about 1% of the peak, (b) angular-dependent sample absorption of the γ-rays and (c) dead-time corrections in the electronics of high counting rates are used. Sample absorption corrections are discussed by Mijnarends (1969) and a somewhat related problem of diffraction of the annihilation photons is discussed by Hyodo, Sueoko & Fujiwara (1971).

A major problem in positron annihilation is the interaction of positrons with vacancies. Although this interaction is proving to be a useful for tool metallurgists in the study of vacancy formation (Seegar, 1973), it can become a serious problem for the study of momentum distributions. Therefore great care must be taken in sample preparation to produce a specimen with a low concentration of vacancies and dislocations. An appreciation of the effects of the positron–vacancy interaction is relatively recent so that much of the early positron data on alloys and polycrystalline metals may be suspect.

V D. Summary

Positron annihilation seems to be best suited for the study of Fermi surfaces in metals and metallic alloys. The excellent resolution, the preferential annihilation of the positron with the outer electrons, the independence of the method on the sample's atomic number, and, in the case of the crossed-slit geometry, the ability to make a one-dimensional cut through the Brillouin zone, make it without rival for this type of study. The problems of positronium formation and the details of the positron wave function are not critical in this case.

As a test of wave functions, positron methods do not have any particular advantage. A detailed knowledge of the positron wave function is important for all materials and in the insulators (from gases to ionic crystals) the problems of positronium formation becomes greater. It is also only just becoming clear to what extent the positron disturbs the electron distribution (Carbotte & Salvadori, 1967; Hede & Carbotte, 1972). These problems however are not necessarily insurmountable and may be solved in the future. Positron methods could then be used to study wave functions for the heavy elements which are now only accessible (barely?) with γ-ray Compton scattering.

VI. Methods of data handling and analysis

VI A. Smoothing methods

When discussing the subject of data smoothing it should be remembered that every method is basically the same, when viewed in the frequency domain, and the choice of one technique over another should be based on convenience, speed, etc, rather than on the belief that one method is, by some magic, intrinsically better than another.

When the data is Fourier transformed and viewed in the frequency domain it is easily seen that at the lower frequencies the signal dominates the noise, and at higher frequency the signal decreases and disappears into the noise. The object of smoothing is then to attenuate the higher-frequency components in some manner so as to gain the smoothest curve with the smallest loss of information. The criterion of 'best curve' is often the χ^2 test (for example see Epstein & Williams, 1973).

A simple and common method of smoothing is the local fitting of a polynomial of low order through some small number of points, usually between three and nine. One such procedure is described by Whittaker & Robinson (1944) and Fortran subroutines using this method are generally available.* This method is local, in the sense it uses only a few points adjacent to the point of smoothing, so that different parts of the data can be smoothed in a different manner if so desired.

A second method of smoothing uses cubic spline functions and is described by Reinsch (1967). This is a global method in the sense that it uses all the points in the interval. The subroutine written by Reinsch works quite well and has the nice feature that each data point can be weighted by its standard deviation.† The major problem with the subroutine is that it requires $\sim 17N$ of computer core to smooth N points.

Another method consists of taking the Fourier transform of the data, attenuating the high-frequency coefficients with some 'cut-off' function, and then taking the inverse transform (Wertheim, 1975). The degree of smoothing depends on the shape of the cut-off function.

The last method to be discussed is the use of low-pass digital filters (Reed & Kaiser, 1975) for smoothing. A digital filter works like an RC filter used for analog data except it is designed to work with digital input. The advantages of this method are speed, small computer core,

it is local and the shape of the filter is known from the three input parameters.

The reader may wonder why the emphasis on global or local nature of the smoothing method. In most cases it makes no difference but in the case of Compton profiles better smoothing can be gained by a local method with the addition of our knowledge of the shape of the profile. We know that near $q = 0$ the profile has sharp features and thus must contain higher frequencies, whereas in the high-q region the data is slowly varying and contains only low frequencies. Thus through the use of a local method the high-q region can be smoothed to a greater degree than the region near $q = 0$ without the loss of information.

No matter what method of smoothing is used the problem should always be viewed in the frequency domain. By knowing both the frequency distribution of the data and the impulse response of the smoothing function the smoothed data can be obtained without unnecessary loss of information.

VI B. Deconvolution

The problem of how to remove the effect of finite spectrometer resolution from experimental data has been discussed by a number of authors [see Inonye, Harper & Rasmussen, (1969); Cheng, Williams & Cooper, (1971) and references quoted therein]. Unfortunately, the existence of noise in the data precludes a 'perfect' solution to the problem.

The best way to view the deconvolution problem is in the frequency domain. It can be shown that if $d(x)$ is the measured data, $r(x)$ is the resolution function, $t(x)$ is the true spectrum and $D(\omega)$, $R(\omega)$ and $T(\omega)$ are the Fourier transforms of d, r and t respectively, then

$$T(\omega) = D(\omega)/R(\omega) \, . \tag{13}$$

If the data were free of noise this would be an exact solution. However, as illustrated by Inonye et al. (1969), the inclusion of noise causes the values of $T(\omega)$ to become large at high ω so that $t(\omega)$ oscillates wildly. Thus the object of the various deconvolution schemes is to attenuate $T(\omega)$ at high frequencies in order to damp the oscillations in $t(x)$, and still retain some of the 'resolution'. This attenuation leads to what has been called the 'residual resolution function' (Paatero et al., 1974) which is essentially the part that is 'forever lost'. Paatero et al. (1974) and Cheng et al. (1971) have discussed and compared the various methods of deconvolution and they will not be discussed here.

The fact that $t(x)$ can never be completely regained from the measured data in the presence of noise raises the question of the most desirable way to present the final results. Presenting only the deconvolved data is inadequate since not all of the resolution has been regained. It is impossible to tell if the differences between the experiment and a theoretical calculation are due to the lost resolution or a deficiency in the theory. A better way of presenting the data is to either present the deconvolved data and an analytic form of the residual resolution function or the data without the correction for resolution and an analytic form of the total resolution function, or both. In this way the theory can be convolved with either of the resolution functions and compared with the data.

VI C. Inversion schemes

Except for the $(e, 2e)$ method, the quantity measured is an integral of the momentum density $n(\mathbf{p})$. Since the momentum density is of considerable interest, inversion schemes

---

* A Fortran IV subroutine *SMOOTH* is available from Mrs. R. C. Cox, Bell Telephone Laboratories, Murray Hill, N.J., U.S.A.

† A Fortran IV version of the subroutine is available from W. A. Reed, Bell Telephone Laboratories, Murray Hill, N.J., U.S.A.

have been developed to invert the integrals to obtain $n(\mathbf{p})$. For Compton scattering and long-slit positron annihilation the integrals are (Mijnarends, 1967)*

$$J(q_z) = \int_{-\infty}^{\infty} \int_{-\infty}^{\infty} n(\mathbf{p}) dp_x dp_y . \qquad (14)$$

For spherically symmetric systems or spherically averaged data (e.g. a gas) the angular integration can be made such that

$$J(q) = 2\pi \int_{q_z}^{\infty} n(p) p\, dp , \qquad (15)$$

and inverting this integral gives the radial momentum density:

$$n(q) = \frac{-1}{2\pi q} \frac{dJ(q)}{dq} . \qquad (16)$$

However for solids, the angular dependence of $J(q)$ can be retained and from measurements made in several crystallographic directions it is then possible to reconstruct the three dimensional $n(\mathbf{p})$.

Currently, three methods have been proposed to invert equation (14). The first and oldest method was developed by Mijnarends (1967) and makes use of Fourier–Hankel transforms. The momentum density is expanded in a series of lattice harmonics $F_l(\theta, \varphi)$ of proper symmetry with coefficient $\varrho_l(\mathbf{p})$. The expansion coefficients are given by

$$\varrho_l(\mathbf{p}) = \frac{-1}{p} \left[\frac{dg_l(p)}{dp} - \frac{l(l+1)}{2p} g_l(p) \right.$$
$$\left. + \frac{1}{p^2} \int_0^p g_l(p_z) P_l''(p_z/p) dp_z \right] ,$$

where $P_l''(p_z/p)$ is the second derivative of the Legendre polynomials. The $g_l(p)$ are determined from the Compton profiles measured along the various crystallographic directions:

$$J_{\alpha, \beta}(q_z) \sim \sum_l g_l(q_z) F_l(\theta, \varphi) ,$$

where α and β refer to the spectrometer coordinates and θ and φ refer to the crystal coordinates (Mijnarends, 1967).

A second method, using Mellin transforms, has been proposed by Majumdar (1971) who considers the inversion of positron annihilation data taken using both the long-slit and crossed-slit geometries. So far this method has not been applied to any experimental data so that its accuracy and general usefulness is unknown.

The third method uses the Fourier transform. In this case $n(\mathbf{p})$ is transformed such that

$$G(\mathbf{r}) \sim \int \exp(i\mathbf{p} \cdot _n) n(\mathbf{p}) d^3p .$$

If only one component of $\mathbf{r}$ is considered then

$$G(r_z) \sim \int \exp(i p_z r_z) J(p_z) dp_z .$$

Thus from profiles measured along a number of crystallographic directions $G(\mathbf{r})$ is determined and then, through the inverse transform, $n(\mathbf{p})$ is obtained. Mueller (1975) has applied this method but with the variations that (a) an

isotropic contribution is subtracted from each profile before applying the transform and (b) a Fourier series is used instead of an integral. Mueller also discusses how the accuracy of $n(\mathbf{p})$ depends upon the number and distribution of the profiles.

It can be shown that for an infinite number of profiles the methods are equivalent (Mijnarends, 1975). However, in practice only a limited number of profiles are available and difference in the calculated $n(\mathbf{p})$ may indeed occur. The differences would be due to the fact that in the Fourier–Hankel method the expansion is fitted to $n(\mathbf{p})$ whereas in the Fourier method the fit is made to the derivative of the Compton profile.

The Fourier–Hankel method has been applied successfully to a number of materials [typical references are Schülke (1974), Kontrym-Sznajd & Stachowiak (1975), Mijnarends (1969, 1971) and Mijnarends & Singru (1974)] whereas so far the Fourier method has only been applied to Si (Mueller, 1975). Thus it is difficult to compare the two methods as applied to actual data. However some general comments can be made that apply to both methods.

The inversion methods are similar to the deconvolution methods used to remove instrumental resolution and suffer from the same problem of noise. To obtain reliable results for $n(\mathbf{p})$ the data must have high statistical accuracy, be taken in as many directions as possible be uniformly distributed over the irreducible part of the Brillouin zone, and be smoothed in some appropriate manner.

A comparison of the speed of the two methods is yet to be determined but it is unlikely that any difference will be of practical significance.* At the present cost of using high-speed computers, even a factor of two would not make the expense of running a significant basis for choice. For example, the program UNFOLD currently runs on a Honeywell-6000 in less than 0·8 minutes.

In summary, it is clear that inversion schemes which calculated $n(\mathbf{p})$ are both practical and useful for the study of momentum distribution and the comparison of theory with experiment. The methods discussed both seem to yield reliable results and only after the same data has been inverted by both methods will it be possible to make a more critical comparison.

VI D. The Lock–Crisp–West theorem

A new approach to the analysis of Compton and positron annihilation data has been proposed by Lock, Crisp & West (1973) to provide a more direct measure of the Fermi surface. They find that

$$F_{ijk}(q) = L_{ijk} \sum_n J_{ijk}(q + n L_{ijk}) ,$$

where q is taken perpendicular to the (ijk) plane whose spacing is L_{ijk}. The function $F_{ijk}(q)$ is thus a constant for each full band, and will reproduce the variation of the cross sectional areas of the Fermi surface in the repeated zone schemes for partially filled bands. This theorem is based on the assumptions that the independent particle approxima-

---

* The following discussion will use Compton scattering notation but is equally valid for positron annihilation [see equation (10)].

* Copies of the program UNFOLD, which uses the Fourier–Hankel method, are available with documentation from P. E. Mijnarends, Reactor Centrum, Nederland, Petten, The Netherlands.

Copies of the program TRIAGE, which uses the Fourier method, are available from F. M. Mueller, Faculty of Science, Catholic Univ., Nijmegen, The Netherlands.

tion is valid, and the Fourier coefficients of the electron wave function (or electron–positron wave function product) be independent of the wave vector **k**. Although this last assumption cannot be strictly correct, Lock *et al.* (1973) argue that the **k** dependence is small enough to allow the approximation to work.

Lock *et al.* (1973) have applied their theorem to some positron annihilation data on Cu and found reasonable agreement with a theoretical calculation. Beardsley, Berko, Nader & Shulman (1975) have also applied this theorem to their own positron data on Cu and to both positron and Compton data on Ge. Their results show that for both Cu and Ge the major features of the theorem are correct. However, they also find deviations from the theoretical prediction which *may* indicate that the approximations made in deriving the theorem are not adequate for highly accurate comparisons. Only further studies with better data will clarify this problem.

VII. Summary

Each of the four experimental techniques discussed has its own particular advantages and disadvantages for measuring electron momentum distributions (Table 1), and should be viewed as a group of complementary techniques. Although each technique has broader application, the following is a list of those areas where each method has a particular advantage.

1. Compton scattering

This technique is probably the most versatile of the four. It can measure gases, liquids and solids, with little regard to atomic number. The resolution is adequate and the time required to make a measurement is reasonable. Despite a number of corrections that must be made to the data, accurate (1 %) Compton profiles are possible. However for any particular experiment, one of the other techniques is quite possibly better, usually due to better resolution.

2. High-energy electron scattering

This technique is best suited for high-resolution measurements in gaseous samples composed of the lighter elements ($z < 10$). It is fast, has excellent resolution and is accurate. However the requirement of gaseous samples of light elements restricts its versatility. The possibility of using thin films could ease these restrictions. In principle it is also possible to study clusters formed in the expanding jet.

3. $(e, 2e)$ scattering

This technique is capable of providing detailed information about the momentum distribution of the valence states of gaseous samples. The resolution is not spectacular and the accuracy of the results is not as good (*per se*) as the other methods. However the lower accuracy is essentially compensated by the fact that $(e, 2e)$ measures the momentum density directly and not an integral of the density. A very attractive feature of the method is that it measures the momentum distributions of each electron orbital separately. The basic restrictions on this method are that the sample must be a gas and only states with low binding energies can be measured.

4. Positron annihilation

Positron annihilation is potentially quite versatile but in practice has concentrated on the study of solids, particularly metals and alloys. This is in part due to the fact that positronium formation is less of a problem but also due to the excellent resolution of the spectrometers. Its ability to detect the sharp break in the momentum distribution due to the Fermi surface and the ability (in the crossed-slit geometry) to look at higher Brillouin zones makes it clearly suited to the study of metals. The question of how the positron wave function disturbs the electron distribution and the exact form of the positron wave function still present problems in using this method to study ground-state wave functions of the sample.

Table 1. *Capsule summary of report*

	X-ray	γ-ray	Electron	Positron	$(e, 2e)$
			Method		
Fundamental	X-ray generator, collimator, analyzer crystal, detectors, recorder, electronics	γ-ray source Ge detector, multichannel analyzer	e-gun, detector, vacuum chamber, signal averager	e^+-source, detectors, spectrometer table, coincidence electronics	e-gun detectors, vacuum chamber, coincidence electronics
Approximate cost (US $)*	$25K	$25–$30K	$25K–$50K	$40K–$75K depending upon geometry	$30K–$40K
Resolution: FWHM compared to FWHM of He	0·20	0·25 with Te source 0·50 with Am source	0·01	0·08	
Samples†	no restrictions except low Z	no restrictions	gases, low Z	no restrictions	gases, low binding energies
Restrictions or problems	multiple scattering, large correction to data	multiple scattering, moderate corrections to data	no solids or liquids	trapping of e^+, form of $\psi^+(r)$	no solids or liquids, relatively low counting rates

* It is not clear how shop costs (*i.e.* labor) were included in these values.
† Z stands for atomic number.

To conclude the report, I want to discuss how the results of a measurement can best be presented in the literature. Some authors present their data only graphically after various corrections have been applied. The net result is that readers are unable to accurately compare any new data or theory with the published results. I therefore suggest that each author publish his data in tabular form; both with and without correction for spectrometer resolution. Although graphs have advantages for illustrating specific points, the basic profiles and anisotropies should be presented in tables on a fine grid if their accuracy is approaching 1%. Tables of data allow other authors to directly compare their data or theory with the published results. The question of deconvoluting the resolution function out of the data is also important. Even with the best detectors the resolution function is a few percent of the momentum distribution so that sharp details of the distribution are smeared. It has also been shown that after deconvolution there is left what is called the 'residual resolution function' (Williams, 1976; Paatero *et al.*, 1974; Cheng *et al.*, 1971) and the original profile cannot be fully recovered. It is therefore useful to the theorist if the data is also published without resolution correction along with the form of the experimental resolution function. The theoretical calculations can then be convoluted with the resolution function for comparison with the data.

A similar comment can be made for theoretical calculations. Not only would tabular data be useful, it would also be novel to see error bars on the calculation. Presumably it is the author who can best judge the uncertainty in the calculated results and this uncertainty should be reflected by some indication of the possible error.

Although this report is issued under the name of only one author, many others have contributed information and ideas. Thus the author takes full responsibility for all errors, misconceptions and inadequacies and gives credit to his associates for the descriptions, evaluations and discussions which they willingly supplied. Special thanks and credit must go to: S. Berko, R. A. Bonham, P. Eisenberger, J. Felsteiner, S. Hosoya, S. M. Kim, I. E. McCarthy, P. E. Mijnarends, F. M. Mueller, T. Paakkari, E. Weigold, R. J. Weiss, H. Wellenstein and B. G. Williams. Without their help this report could not have been written.

References

BEARDSLEY, G. M., BERKO, S., MADER, J. J. & SHULMAN, M. A. (1975). *Appl. Phys.* 5, 375–378.

BERKO, S. & MADER, J. (1975). *Appl. Phys.* 5, 287–306.

BERKO, S. & PLASKETT, J. Sl. (1958). *Phys. Rev.* 112, 1877–1887.

BONHAM, R. A. (1969). *Rec. Chem. Progr.* 30, 185–208.

BONHAM, R. A. & FINK, M. (1974). *High Energy Electron Scattering*, Chap. 5 & 6. New York: Van Nostrand Reinhold.

BONHAM, R. A. & TAVARD, C. (1973). *J. Chem. Phys.* 59, 4691–4704.

BONHAM, R. A. & WELLENSTEIN, H. F. (1973a). *Int. J. Quantum Chem. Symp.* No. 7, 377–394.

BONHAM, R. A. & WELLENSTEIN, H. F. (1973b). *J. Appl. Phys.* 44, 2631–2634.

BONHAM, R. A. & WELLENSTEIN, H. F. (1975a). Private communication.

BONHAM, R. A. & WELLENSTEIN, H. F. (1975b). *Electron Spectroscopy: Theory, Techniques and Applications.* Edited by C. R. BRUNDLE & A. D. BAKER. London: Academic Press. To be published.

CAMILLONI, R., GIARDINI-GUIDONI, A., TIRIBELLI, R. (1972). *Phys. Rev. Lett.* 29, 618–621.

CARBOTTE, J. P. & SALVADORI, A. (1967). *Phys. Rev.* 162, 290–300.

CHENG, R., WILLIAMS, B., & COOPER, M. (1971). *Phil. Mag.* 23, 115–133.

COOPER, M. (1971). *Advanc. Phys.* 20, 453–491.

DAUWE, C., DORIKENS-VANPRAET, L. & DORKINS, M. (1972). *Solid State Commun.* 11, 717–720.

DEKHTYAR, I. YA. (1974). *Phys. Rep.* 9, 243–353.

DEY, S., McCARTHY, I. E., TEUBNER, P. J. O. & WEIGOLD, E. (1975). *Phys. Rev. Lett.* 34, 782–785.

EHRHARDT, H., HESSELBACHER, K. H., JUNG, K. & WILLMANN, K. (1972). *J. Phys.* (B), 5, 1559–1571.

EHRHARDT, H., SCHULZ, M., TAKAAT, T. & WILLMA, K. (1969). *Phys. Rev. Lett.* 22, 89–92.

EISENBERGER, P. (1970). *Phys. Rev.* (A), 2, 1678–1686.

EISENBERGER, P. (1972). *Phys. Rev.* (A), 5, 628–635.

EISENBERGER, P. & PLATZMAN, P. M. (1971). *Phys. Rev.* (A), 2, 415–423.

EISENBERGER, P. & REED, W. A. (1972). *Phys. Rev.* (A), 5, 2085–2094.

EISENBERGER, P. & REED, W. A. (1974). *Phys. Rev.* (B), 9, 3237–3241.

EPSTEIN, I. & WILLIAMS, B. (1973). *Phil. Mag.* 27, 311–328.

FELSTEINER, J. & PATTISON, P. (1975). *Nucl. Instrum. Meth.* 124, 449–453.

FELSTEINER, J., PATTISON, P. & COOPER, M. (1974). *Phil. Mag.* 30, 537–546

FUJIWARA, K. & SUEOKA, O. (1966). *J. Phys. Soc. Japan*, 21, 1947–1955.

FUKAMACHI, T. & HOSOYA, S. (1972). *Phys. Lett.* (A), 38, 341–342.

FUKAMACHI, T. & HOSOYA, S. (1973). *Phys. Stat. Sol.* (A), 15, 629–634.

FURNESS, J. B. & McCARTHY, I. E. (1973). *J. Phys.* (B), 6, 2280–2291.

FURNESS, J. B. & McCARTHY, I. E. (1974). *J. Phys.* (B), 7, 541–547.

GUSTAFSON, D. R., MACKINTOSH, A. R. & ZAFFARANO, D. J. (1963). *Phys. Rev.* 130, 1455–1459.

HEDE, B. B. J. & CARBOTTE, J. P. (1972). *J. Phys. Chem. Solids*, 33, 727–735.

HOOD, S. T., McCARTHY, I. E., TEUBNER, P. J. O. & WEIGOLD, E. (1973). *Phys. Rev.* (A), 8, 2494–2500.

HOOD, S. T., McCARTHY, I. E., TEUBNER, P. J. O & WEIGOLD, E. (1974). *Phys. Rev.* (A), 9, 260–266.

HOSOYA, S. (1974). *Diffraction Studies of Real Atoms and Real Crystals.* Int. Crystallogr. Conf., Melbourne. Australian Academy of Science.

HOTZ, H. P., MATHIESEN, J. M. & HURLOY, J. P. (1968). *Phys. Rev.* 170, 351–355.

HOWELLS, M. R. & OSMON, P. E. (1972). *J. Phys.* (E), 2, 277–288.

HUGHES, A. C. & MANN, M. M. (1938). *Phys. Rev.* 53, 50–63.

HYODO, T., SUEOKA, O. & FUJIWARA, K. (1971). *J. Phys. Soc. Japan*, 31, 563–573.

INONYE, T., HARPER, T. & RASMUSSEN, N. C. (1969). *Nucl. Instrum. Meth.* 67, 125–132.

IONKUTI, M. (1971). *Rev. Mod. Phys.* 43, 297–347.

KIM, S. M. & BUYERS, W. J. L. (1972). *Canad J. Phys.* **50**, 1777–1781.

KOLLATH, R. (1936). *Ann. Phys.* **27**, 721–741.

KONTRYM-SZNAJD, G. & STACHOWIAK, H. (1975). *Appl. Phys.* **5**, 361–365.

LANGHOFF, P. W. & SEIDMAN, S. L. (1974). *Chem. Phys. Lett.* **27**, 195–198.

LASSETTRE, A. E. N. & SKERBELA, A. (1974). *Methods of Experimental Physics*, edited by D. WILLIAMS. Vol. 3B, Chapter 7·2. New York: Academic Press.

LOCK, D. G., CRISP, V. H. C. & WEST, R. H. (1973). *J. Phys. (F)*, **3**, 561–570.

McCARTHY, I. E. (1973). *J. Phys. (B)*, **6**, 2358–2367.

MAJUMDAR, C. H. K. (1971). *Phys. Rev. (B)*, **4**, 2111–2115.

MANNINEN, S., PAAKKARI, T. & KAJANTIE, K. (1974). *Phil. Mag.* **29**, 167–178.

MIJNARENDS, P. E. (1967). *Phys. Rev.* **160**, 512–519.

MIJNARENDS, P. E. (1969). *Phys. Rev.* **178**, 622–629.

MIJNARENDS, P. E. (1971). *Phys. Rev. (B)*, **4**, 2820–2822.

MIJNARENDS, P. E. (1973). *Physica*, **63**, 235–247.

MIJNARENDS, P. E. (1975). To be published.

MIJNARENDS, P. E. & SINGRU, R. M. (1974). *Appl. Phys.* **4**, 303–306.

MUELLER, F. M. (1975). To be published.

PAATERO, P., MANNINEN, S. & PAAKKARI, T. (1974). *Phil. Mag.* **30**, 1281–1294.

PATTISON, P., MANNINEN, S., FELSTEINER, J. & COOPER, M. (1974). *Phil. Mag.* **30**, 973–984.

PHILLIPS, W. C. & WEISS, R. J. (1968). *Phys. Rev.* **171**, 790–800.

PLATZMAN, P. M. & TZOAR, N. (1965). *Phys. Rev.* **139**, 410–413.

PLATZMAN, P. M. & TZOAR, N. (1970). *Phys. Rev. (B)*, **2**, 3556–3559.

RACHINGER, W. A. (1968). *J. Sci. Instrum.* **25**, 254–255.

RAMA-REDDY, K. & CARRIGAN, R. A. (1970). *Nuovo Cim.* **663**, 195–118.

REED, W. A. & KAISER, J. F. (1975). To be published.

REINSCH, C. H. (1967). *Numer. Math.* **10**, 177–183.

RIBBERFORS, R. (1975). *Phys. Rev. (B)*, **12**, 2067–2074.

SCHMORANZER, H., WELLENSTEIN, H. F. & BONHAM, R. A (1975). *Rev. Sci. Instrum.* **46**, 89–91.

SCHÜLKE, W. (1974). *Phys. Stat. Sol. (B)*, **62**, 453–460.

SEEGAR, A. (1973). *J. Phys. (F)*, **3**, 348–294.

STROUD, D. & EHRENREICH, H. (1968). *Phys. Rev.* **171**, 399–407.

SUEOKA, O. (1967). *J. Phys. Soc. Japan*, **23**, 1246–1250.

TANIGAWA, S., NANAO, S., KURIBAYASHI, K. & DOYAMA, M. (1971). *J. Phys. Soc. Japan*, **31**, 1689–1694.

TAVARD, C. & BONHAM, R. A. (1969). *J. Chem. Phys.* **50** 1736–1747.

UGBABE, A., WEIGOLD, E. & McCARTHY, I. E. (1975). *Phys. Rev. (A)*, **11**, 576–585.

WEIGOLD, E., HOOD, S. T. & McCARTHY, I. E. (1975). *Phys. Rev. (A)*, **11**, 566–575.

WEISS, R. J., HARREY A. & PHILLIPS, W. C. (1968). *Phil. Mag.* **17**, 241–253.

WIEL, M. J. VAN DER & BRIAN, C. E. (1972). *J. Electron Spectrosc.* **1**, 309–318.

WELLENSTEIN, H. F. (1973). *J. Appl. Phys.* **44**, 3669–3674.

WELLENSTEIN, H. F. & BONHAM, R. A. (1973). *Phys. Rev. (A)*, **7**, 1568–1572.

WELLENSTEIN, H. F., BONHAM, R. A. & ULSH, R. C. (1973). *Phys. Rev. (A)*, **8**, 304–314.

WELLENSTEIN, H. F., SCHMORANZER, H., BONHAM, R. A., TUCK, C. & LEE, J. S. (1975). *Rev. Sci. Instrum.* **46**, 92–97.

WERTHEIM, G. K. (1975). *Rev. Sci. Instrum.* **46**, 1414–1415.

WEST, R. N. (1973). *Advanc. Phys.* **22**, 263–383.

WHITTAKER, E. T. & ROBINSON, G. (1944). *The Calculus of Observations*, pp. 285–289. London: Blackie.

WILLIAMS, B. (1976). *Acta Cryst.* A**32**, 513–526.

WILLIAMS, B. & HALONEN, V. (1975). *Phys. Fenn.* **10**, 5–20.

WILLIAMS, D. L., BECKER E. H., PETIJEVICH, P. & JONES, G. (1968). *Phys. Rev. Lett.* **20**, 448–450.